

## Time reversal of optical nutation signals

Y. S. Bai, A. G. Yodh, and T. W. Mossberg

*Department of Physics, Harvard University, Cambridge, Massachusetts 02138*

(Received 3 March 1986)

Optical nutation signals are found to be modified in interesting ways by a short, intense, excitation pulse. In particular, pulses of appropriate character are found to effect a time reversal of the optical nutation signal, i.e., the nutation signal after the short pulse evolves as the mirror image of the nutation signal before the pulse. In ideal cases, all dephasing effects resulting from inhomogeneous broadening are reversed, and a nutation echo occurs when all atoms rephase in the *excited* state. Various excitation conditions that lead to the time reversal of optical nutation signals are considered, and numerical simulations are compared with experimental results. Finally, the rephasing considered here is compared to that observed in the case of rotary echoes.

### I. INTRODUCTION

When a two-level atom is exposed to a step-function, nearly resonant driving field, it executes Rabi oscillations back and forth between its ground and excited states alternately depleting and enhancing the strength of the driving field in the process. The latter effect is manifest in the oscillations observed in the transmission of a step-function light pulse through an atomic ensemble. Such oscillations are referred to as optical nutation signals,<sup>1-6</sup> and can be observed whenever the Rabi oscillation period is comparable to or shorter than the homogeneous atomic relaxation time. Even when the homogeneous relaxation can be ignored, however, the number of oscillations that can be observed in an optical nutation signal is limited by damping introduced by the strong inhomogeneous dephasing which is found in most optical systems. The presence of this strong damping limits the utility of optical nutation signals in studies of weak homogeneous relaxation.

In this paper we report on the effect of applying a short, intense pulse in the midst of the optical nutation process. Such pulses can effect a reversal of the inhomogeneous-broadening-induced damping of the optical nutation signal and, concomitantly, induce a rephasing of the atoms in their excited state. After application of an appropriate pulse, the nutation signal grows in amplitude displaying a mirror image of its behavior before the pulse. Upon regaining its original amplitude (ignoring homogeneous decay), the nutation signal experiences an abrupt phase reversal, and then resumes its decay. The phase reversal signifies the rephasing of the precessing atoms in their excited state. Being free from the effects of inhomogeneous-broadening mechanisms, the excited-state rephasing signal constitutes an excellent means of studying various homogeneous relaxation processes.

In the following, we analytically investigate the nutation signal expected in various simple cases, provide numerical simulations appropriate to more complicated short-pulse conditions, and discuss pulse-modified optical nutation in a time-dependent driving field. Our calculations are compared with the results of experiments conducted in atomic Yb vapor. Finally, we compare pulse-induced rephasing of nutation signals with that observed in rotary echo experiments.<sup>7-10</sup> The latter are generated

by suddenly introducing a 180° shift in the driving field's phase.

### II. OPTICAL NUTATION

We start by considering a single two-level atom that has a transition frequency  $\omega$ , and interacts with a laser field of the form

$$E(z,t) = \frac{E_0}{2} \exp[i(\omega_0 t - kz + \phi_d)] + \text{c.c.}, \quad (1)$$

where  $E_0$  represents a constant real field amplitude. The atom's response to this field is described by the well-known optical Bloch equations.<sup>1</sup> Neglecting homogeneous damping terms and working in the rotating frame, the Bloch equations can be written in vector form as

$$\frac{d}{dt} \mathbf{R} = \boldsymbol{\Omega} \times \mathbf{R}, \quad (2a)$$

where the atomic state vector  $\mathbf{R}$  and the driving field vector  $\boldsymbol{\Omega}$  are given by

$$\mathbf{R} = (u, v, w) \quad (2b)$$

and

$$\boldsymbol{\Omega} = (-\chi_0, 0, \Delta), \quad (2c)$$

respectively. Here  $\chi_0 = pE_0/\hbar$  is the Rabi frequency associated with the atom-field system,  $p$  is the atomic dipole moment,  $\Delta = \omega - \omega_0$  represents the detuning of the atom from the laser central frequency, and  $u, v, w$  have their usual definitions in terms of the atomic density matrix.<sup>1,4</sup> Using Eq. (2), we see that the atomic state vector will precess about the driving-field vector as shown in Fig. 1.

Since the driving field is of constant amplitude, Eq. (2) can be solved analytically.<sup>1,4</sup> If we assume that the atom is in its ground state at the time  $t=0$  when the driving field is turned on, i.e.,  $\mathbf{R}(0) = (0, 0, -1)$ , the atomic-state vector components for  $t > 0$  are given by

$$u = \frac{\Delta \chi_0 [1 - \cos(\Omega t)]}{\Omega^2}, \quad (3a)$$

$$v = -\frac{\chi_0 \sin(\Omega t)}{\Omega}, \quad (3b)$$

and

$$w = -\frac{\Delta^2 + \chi_0^2 \cos(\Omega t)}{\Omega^2}. \quad (3c)$$

Here  $\Omega = (\chi_0^2 + \Delta^2)^{1/2}$ .

We now consider an optically thin ensemble of atoms of the type described above, but having a distribution of detunings  $\Delta$ . Once exposed to the driving field [see Fig. 2(a) for a schematic of the excitation sequence], the atoms collectively radiate a field of the form

$$E(z, t) = \frac{E_{s0}}{2} \exp[i(\omega_0 t - kz)] + c.c. \quad (4a)$$

The complex field amplitude  $E_{s0}$  is given by<sup>4</sup>

$$E_{s0} = ia_0 \int_{-\infty}^{\infty} (u + iv) g(\Delta) d\Delta \equiv ia_0 \langle u + iv \rangle, \quad (4b)$$

where  $a_0$  is a real constant and  $g(\Delta)$ , assumed symmetric about  $\Delta = 0$ , represents the distribution of detunings. The light field after the sample consists of the coherent sum of the driving and sample fields. Its intensity is given approximately by

$$\begin{aligned} I_d(t) &\simeq I_0 [1 + 2 \operatorname{Re}(E_{s0})/E_0] \\ &= I_0 [1 - 2a_0 \langle v \rangle / E_0], \end{aligned} \quad (5)$$

where  $I_0$  is the intensity of the driving field, we have assumed that  $|E_0| \gg |E_{s0}|$  (optically thin sample), and  $\langle \rangle$  represents the  $\Delta$  average as above. As described elsewhere,<sup>4</sup> in the limit that  $g(\Delta)$  can be considered constant, the oscillatory part of  $I_d(t)$  is a Bessel's function. This is the standard optical nutation signal.

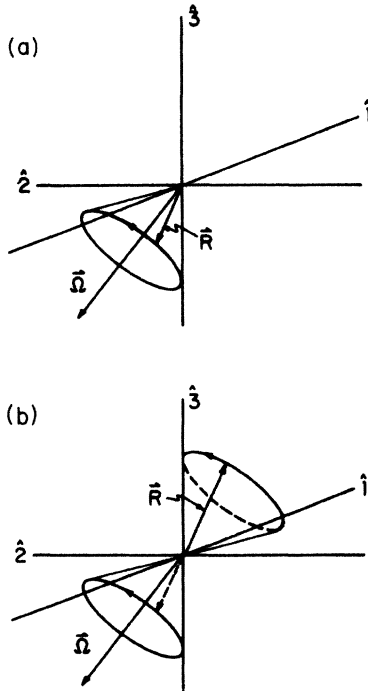


FIG. 1. (a) Atomic state vector  $\mathbf{R}$ , precessing about driving-field vector  $\Omega$  according to Eq. (2) of text. (b) Motion of  $\mathbf{R}$  in the constant driving field after experiencing a short-pulse-induced  $180^\circ$  rotation about the 2 axis.

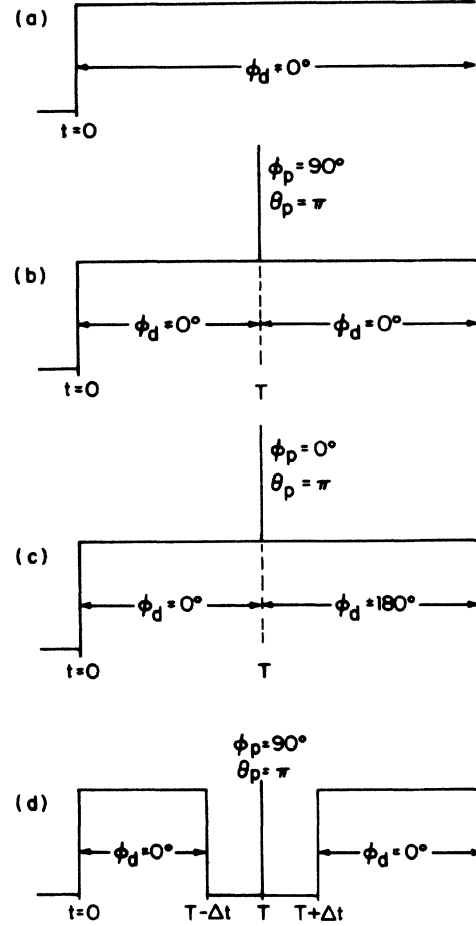


FIG. 2. Schematic of several excitation sequences discussed in the text. The horizontal axis corresponds to time, and the vertical axis to the strength of the excitation fields.  $\phi_d$ , phase of driving field;  $\phi_p$ , phase of short excitation pulse;  $\theta_p$ , pulse area of short pulse. (a) Excitation for standard optical nutation signals. (b) Excitation sequence for pulse-induced nutation echoes as discussed in case 1 of the text. (c) Excitation sequence for case 2 of the text in which the phase of the driving field is varied. (d) Excitation sequence for case 3 of text in which the amplitude of the driving field is time dependent.

### III. TIME-REVERSED OPTICAL NUTATION

Case 1: Constant driving field [see Fig. 2(b)]. Suppose that a short, intense pulse,  $90^\circ$  out of phase with respect to the driving field and of area  $\pi$ , is applied at a time  $t = T$ . The effect of the pulse is to suddenly rotate the atomic state vectors  $180^\circ$  about the  $v$  axis [see Fig. 1(b)]. It follows that the atomic state vectors immediately after ( $t = T^+$ ) and before ( $t = T^-$ ) the short pulse are related according to

$$\mathbf{R}(T^+) = (-u(T^-), v(T^-), -w(T^-)). \quad (6)$$

A solution for  $\mathbf{R}(t > T)$  consistent with the value of  $\mathbf{R}(T^+)$  in Eq. (6) is given by

$$u = -\frac{\Delta\chi_0\{1 - \cos[\Omega(2T - t)]\}}{\Omega^2}, \quad (7a)$$

$$v = -\frac{\chi_0\sin[\Omega(2T - t)]}{\Omega}, \quad (7b)$$

$$w = \frac{\Delta^2 + \chi_0^2\cos[\Omega(2T - t)]}{\Omega^2}. \quad (7c)$$

This solution has several interesting features. First,  $\langle v \rangle$  is symmetric about  $t=T$  and changes sign at  $t=2T$ . This implies that the optical nutation signal for  $T < t < 2T$  is the time-reverse of the signal for  $t < T$ . Second,  $w(t=2T)=1$  regardless of atomic detuning  $\Delta$ , i.e., at  $t=2T$  all atoms rephase in the excited state. We refer to this effect as a pulse-induced nutation echo.

Case 2: Variable-phase driving field [see Fig. 2(c)]. Let a driving field and a short  $\pi$  pulse be applied at the times described above. This time, however, assume that the short pulse and the driving field ( $t < T^-$ ) have the same phase, but that the driving field experiences a sudden  $180^\circ$  phase shift at  $t=T^+$ . In this case, we have

$$\mathbf{R}(T^+) = [u(T^-), -v(T^-), -w(T^-)]. \quad (8)$$

A solution for  $\mathbf{R}(t > T)$  that is consistent with  $\mathbf{R}(T^+)$  above is given by Eq. (7) modified only by an overall sign change in the expressions for  $u$  and  $v$ . In other words, a pulse-induced nutation echo also occurs with this excitation scheme. Since  $E_{s0} \propto \langle v \rangle$  and  $E_0$  both change sign for  $t > T$ , the optical nutation signal is still symmetric about  $t=T$  even though  $\langle v \rangle$  is not.

Case 3: Driving field with a time-dependent amplitude [see Fig. 2(d)]. When the driving field has a time-dependent amplitude, simple analytic expressions for the behavior of the atomic state vector are no longer possible. We simply point out that the short pulses described above should time reverse the optical nutation quite generally provided that the magnitude of the driving field is symmetric about  $t=T$ . This can be seen in the vector model picture by following an arbitrary ground-state (excited-

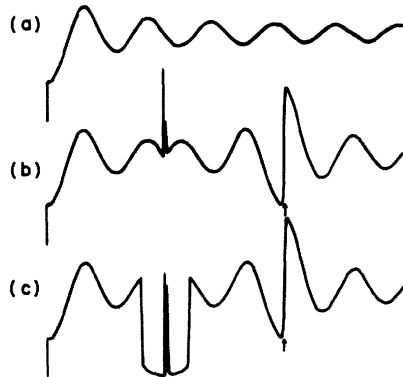


FIG. 3. Results of our computer calculations of (a) a simple optical nutation signal, (b) pulse-induced nutation echo in a constant driving field (case 1), and (c) pulse-induced nutation echo (case 3) where the amplitude of the driving field is time dependent. See text for conditions. The arrow indicates the pulse-induced nutation echo.

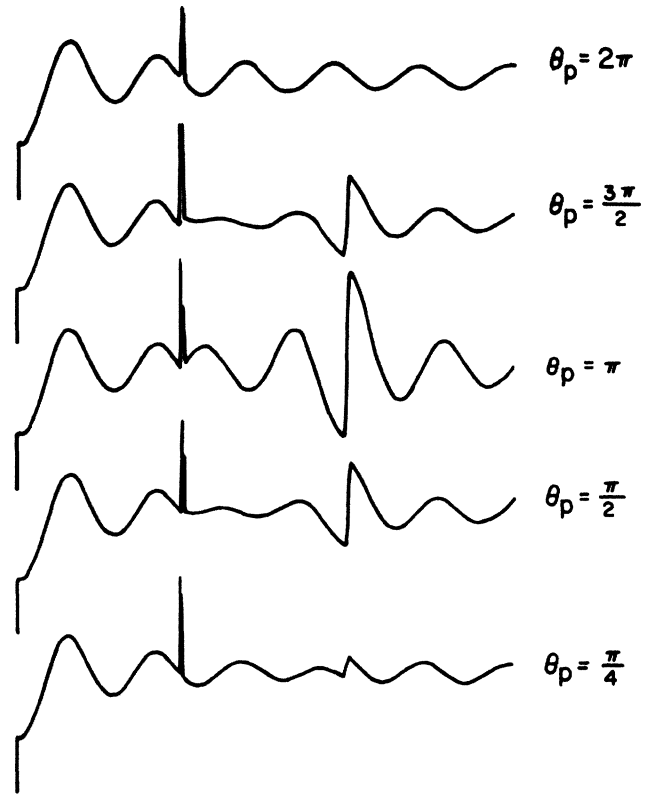


FIG. 4. Simulations of pulse-induced nutation echoes (case 1) generated with various short pulse areas,  $\theta_p$ . All other conditions are the same as in Fig. 3(b).

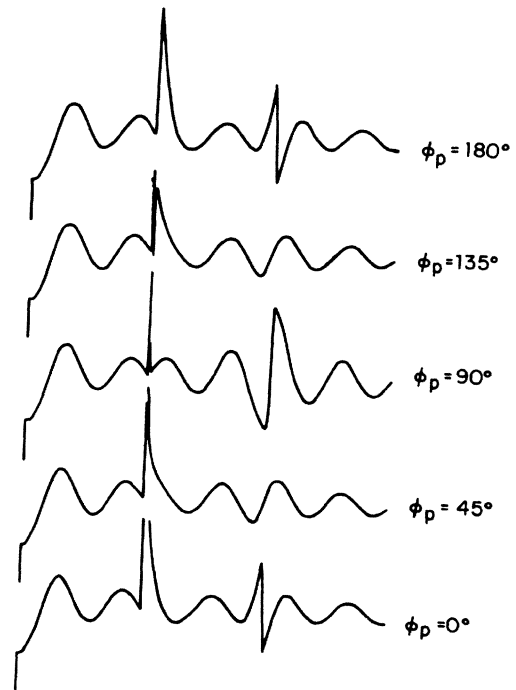


FIG. 5. Simulations of pulse-induced nutation echoes (case 1) generated with short pulses of various phase shifts,  $\phi_p$ , relative to the driving field. All other conditions are the same as in Fig. 3(b).

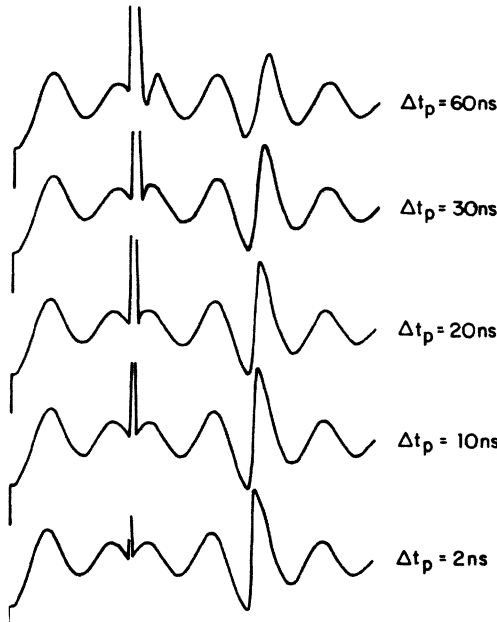


FIG. 6. Simulations of pulse-induced nutation echoes (case 1) for various temporal durations  $\Delta t_p$  of the short pulse. In these calculations we have kept the short-pulse area constant, and equal to  $\pi$  for atoms that are exactly on resonance ( $\Delta=0$ ).

state) atom forward in time from  $t=0$  (backward in time from  $t=2T$ ), and seeing that the short pulse rotates one state vector into the other.

We have performed numerical simulations of the optical nutation signal appropriate to the simple cases described above and to more general cases in which the area, phase shift, and duration of the short pulse vary. Unless specified otherwise, the calculations were performed under the following conditions: (1) The inhomogeneous absorption profile of the sample was taken as Gaussian with a full width at half maximum of 100 MHz; (2) the short-pulse temporal duration was 2 ns, and the short-pulse area was determined from the precession angle of an atom exactly on resonance ( $\Delta=0$ ); (3) the steady-state unsaturated absorption of the sample was 50%; (4) the driving-field Rabi frequency was 3.8 MHz, and (5) the total time for all simulations was 1500 ns, significantly

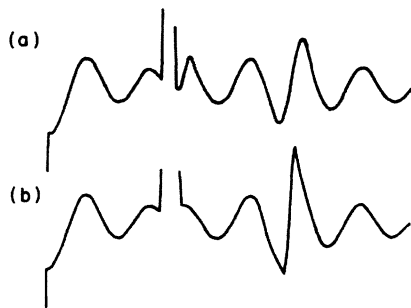


FIG. 7. Simulations of pulse-induced nutation echoes with long rephasing pulses ( $\Delta t_p = 60$  ns) of different areas. (a)  $\theta_p = \pi$ . (b)  $\theta_p = 11\pi$ .

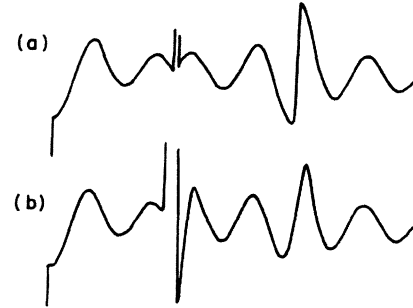


FIG. 8. Simulations of pulse-induced nutation echoes generated according to the excitation scheme of case 2. (a)  $\Delta t_p = 2$  ns. (b)  $\Delta t_p = 60$  ns.

less than the reciprocal of the frequency steps used in the numerical integrations over detunings.

In Figs. 3–8, we present the results of our calculations. In each case, the figure represents the intensity of the light transmitted through the sample versus time. In all the simulations, the nutation actually begins with a short interval of high transmission of the driving field through the sample. This feature arises from the finite (100 MHz) bandwidth employed in the calculations and has been suppressed in the figures. In Fig. 3(a), we show an optical nutation signal unaffected by a short excitation pulse. Below it, in part (b) of the figure we show a nutation echo produced under the excitation conditions described in case 1 above. The abrupt change in the nutation signal at  $t=2T$  corresponds to a change in sign of  $\langle v \rangle$  as all of the atoms pass through the excited state. In Fig. 3(c) a trace generated assuming a driving field of time-dependent amplitude but constant phase is presented. As discussed in case 3 above, the optical nutation signal is still symmetric about the short pulse. In Figs. 4 and 5, we show, respectively, the effect of varying the area and the phase of the short pulse. In Fig. 6, we examine the effect of non-negligible  $\pi$ -pulse duration, and find that increasing duration leads primarily to a smoothing of the abrupt rephasing feature. This smoothing is, of course, related to the fact that longer  $\pi$  pulses rephase atoms over a narrower bandwidth. In Fig. 7, we show that by increasing the intensity (area) of a long rephasing pulse one can reduce the smoothing effect just mentioned. At the higher pulse intensity, atoms over a larger bandwidth experience a net  $180^\circ$  rotation of their state vectors. For completeness, in Fig. 8 we show a simulation of a pulse-induced nutation echo generated according to the excitation scheme of case 2. Longer pulses of constant area are found to lead as expected to a smoothing of the rephasing as seen also in Fig. 6.

#### IV. EXPERIMENT

In our experiment (see Fig. 9), acousto-optical modulators (rise time 20 ns) were employed to generate optical pulses of variable amplitude and duration by gating the output of a single-mode cw ring dye laser. A series of two modulators was employed to achieve the necessary on-to-off contrast ratio. The phases of the pulses were con-

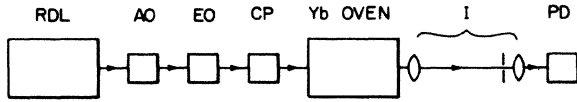


FIG. 9. Schematic of experimental setup. RDL, ring dye laser; AO, acousto-optical modulator; EO, electro-optical modulator; CP, circular polarization optics; I, imaging optics; PD, photodetector.

trolled by passing them through an electro-optical modulator (switching time 10 ns). The experiments were conducted on the 555.6-nm  $(6s^2)^1S_0-(6s6p)^3P_1$  transition (upper-state lifetime 875 ns) of atomic  $^{174}\text{Yb}$ . The Yb was housed in a stainless-steel vapor cell with a 5-cm active vapor length. The cell was maintained at a constant temperature of about 750 K to produce a weak signal absorption of 50% at line center. The absence of a hyperfine interaction in  $^{174}\text{Yb}$  allowed us to realize ideal two-level atomic response by employing circularly polarized excitation fields and applying a 65-G axial magnetic field throughout the sample. The laser beam was collimated with a 1 mm diameter as it traversed the Yb vapor region. Optics were employed to image signals generated in only the central portion of the laser beam's spatial profile onto the detector. In this way, a damping of the nutation signal due to a spread of Rabi frequencies across the beam profile was avoided. In the detected region, laser intensity variations are estimated to be less than 5%. The signal was detected using a fast silicon photodiode (rise time less than 1 ns) and recorded by a boxcar integrator. Throughout the experiment, the short pulse was 30 ns in duration. Its phase was controlled by the application of a voltage pulse of 40 ns width to the electro-optical modulator. In cases where the phase of the driving field was changed, a step-function voltage pulse was applied to the modulator.

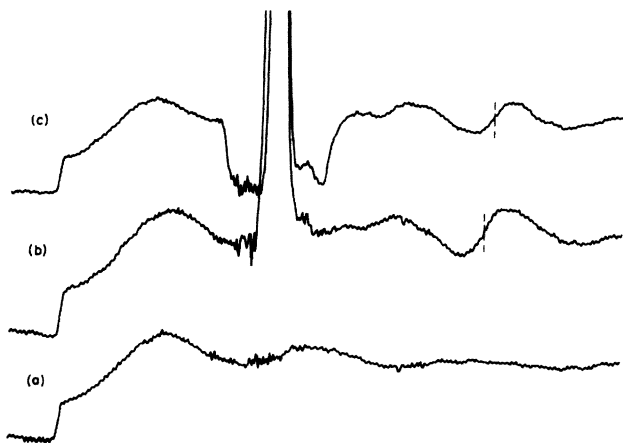


FIG. 10. Experimental results of (a) simple optical nutation, (b) pulse-induced nutation echo (case 1), (c) pulse-induced nutation echo with time-dependent driving field (case 3). In all cases, the total time elapsed from start to finish of a trace is 1400 ns. Dashed lines indicate rephasing point.

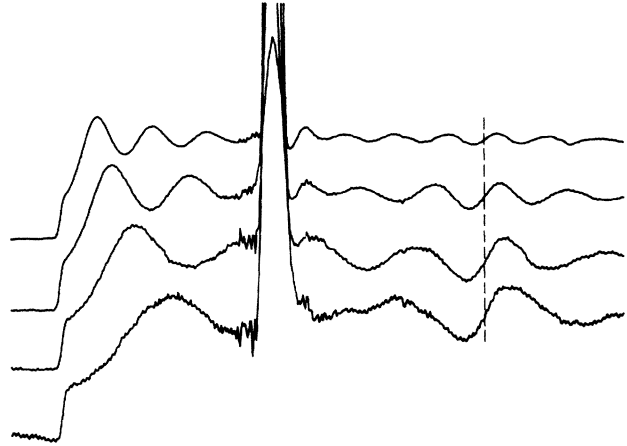


FIG. 11. Experimental pulse-induced nutation echoes (case 1) as a function of driving-field intensity. Dashed line indicates common rephasing point.

In Figs. 10(a) and 10(b), respectively, we show a simple nutation signal and a nutation echo (case 1) generated by a short pulse adjusted to have roughly a  $90^\circ$  phase shift and an echo-optimizing intensity. The calculated short-pulse area in the latter case is approximately  $\pi$ . The observed signal closely resembles the traces shown in Fig. 6. In Fig. 10(c), we show a trace in which the magnitude of the driving field is time dependent but symmetric about the short pulse. As described in case 3 above and simulated in Fig. 3(c), the optical nutation signal is again time-reversed about the short pulse. In Fig. 11, we show a series of nutation echo traces generated as in Fig. 10(b) but with various driving-field intensities. The symmetry about the rephasing point and the short pulse is manifest. In Fig. 12, we show a nutation echo generated under the excitation conditions described in case 2 above. Finally, for contrast we show a rotary echo in Fig. 13. This signal is generated without a short pulse by simply introducing a  $180^\circ$  phase shift in the driving field.

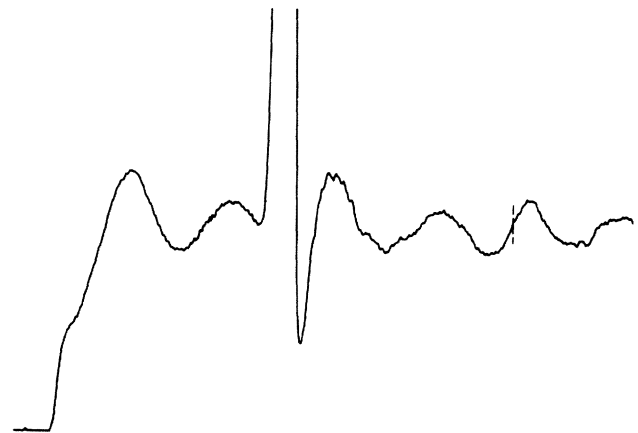


FIG. 12. Experimental pulse-induced nutation echo generated under excitation conditions of case 2 in text. Dashed line indicates rephasing point.

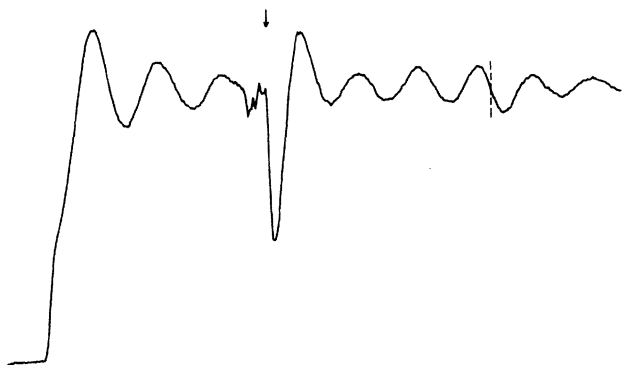


FIG. 13. Rotary echo generated experimentally by switching the phase of the driving field by  $180^\circ$  at the time indicated by the arrow above. Dashed line indicates rephasing point.

### V. COMPARISON WITH ROTARY ECHO

The dynamics of the rotary echo are quite simple.<sup>7-10</sup> Consider an optical nutation sequence in which the phase of the driving field is shifted by  $180^\circ$  at some time  $T$  after the onset of nutation at  $t=0$ . We assume that atomic detunings are small compared to the Rabi frequency, i.e.,  $\chi_0 \gg \Delta$ , but allow for a variation of  $\chi_0$  throughout the sample. Under these conditions, the phase shift changes the sign of  $\Omega$ , and for  $t > T$ , the atomic state vectors precess about the same cones as for  $t < T$ , see Fig. 1(a), but in the opposite sense. At  $t=2T$ , all atoms will rephase in the *ground* state regardless of the local magnitude of  $\chi_0$ .

When  $\Delta$  cannot be neglected compared to  $\chi_0$ , the phase shift does not reverse  $\Omega$  exactly, and complete rephasing does not occur. The rotary echo is very efficient at reversing dephasing attributable to spatial inhomogeneity of  $\chi_0$ , but not that resulting from inhomogeneous broadening. In the case of pulse-induced nutation echoes, the field-strength requirement is transferred from the driving field to the short pulse. Provided that  $\chi_p$ , the short pulse Rabi frequency, is much greater than the relevant spread of  $\Delta$ 's complete rephasing can occur regardless of the size of  $\chi_0$ . Another interesting difference between rotary-echo and pulse-induced rephasing is that the former occurs in the *ground* state while the latter occurs in the *excited* state.

### VI. CONCLUSION

We have pointed out a novel new type of rephasing that occurs when a short pulse is applied during the optical nutation process. This effect produces rephasing of a broader set of atoms than are rephased in rotary echoes, and should be useful in relaxation studies.

### ACKNOWLEDGMENTS

This work was supported by the National Science Foundation Grant No. PHY-85-04260 and the Joint Services Electronics Program Grant No. N00014-84-K-0465. It was made possible by an equipment grant from the Department of Defense University Research Instrumentation Program Grant No. DAAG-29-84-G-0012. A. G. Y. acknowledges the support of the U. S. Army.

<sup>1</sup>L. Allen and J. H. Eberly, *Optical Resonance and Two-Level Atoms* (Wiley, New York, 1975).

<sup>2</sup>G. B. Hocker and C. L. Tang, *Phys. Rev. Lett.* **21**, 591 (1968).

<sup>3</sup>R. G. Brewer and R. L. Shoemaker, *Phys. Rev. Lett.* **27**, 631 (1971).

<sup>4</sup>R. G. Brewer, in *Frontiers in Laser Spectroscopy, Les Houches, session XXVII*, edited by R. Balian, S. Haroche, and S. Liberman (North-Holland, Amsterdam, 1977), Vol. 1.

<sup>5</sup>P. M. Farrell, W. R. Macgillivray, and M. C. Standage, *Phys. Lett.* **107A**, 263 (1985).

<sup>6</sup>R. L. Shoemaker and E. W. Van Stryland, *J. Chem. Phys.* **64**, 1733 (1976).

<sup>7</sup>I. Solomon, *Phys. Rev. Lett.* **2**, 301 (1959).

<sup>8</sup>N. C. Wong, S. S. Kano, and R. G. Brewer, *Phys. Rev. A* **21**, 260 (1980).

<sup>9</sup>T. Muramoto, S. Nakanishi, O. Tamura, and T. Hashi, *Jpn. J. Appl. Phys.* **19**, L211 (1980).

<sup>10</sup>F. Rohart, P. Glorieux, and B. Macke, *J. Phys. B* **10**, 3835 (1977).